Applying the refraction migration method to image a deep interface in Xinjiang, China

Yang Shen, Jie Zhang, University of Science and Technology of China (USTC)*

Summary

Seismic interferometry is an effective approach in solving imaging problems. By applying a seismic interferometry method, one can obtain virtual reflection records between any two adjacent receivers from refractions, and then apply migration to the virtual reflection records for imaging. To ensure the imaging result accurate, we should utilize a large number of virtual reflections to stack and cancel out invalid events. In this study, we apply the refraction migration method to image a deep interface in Xinjiang, China by processing long offset refractions. For further improving the feasibility of the method, we employ the super-virtual interferometry to enhance the far offset refractions before creating virtual refractions. Real data test demonstrates that this approach is promising for processing the long-offset record for imaging deep interfaces. The method is especially useful when reflections in the data are too weak or missing, since refractions are almost always available.

Introduction

Interferometry has been extensively studied and applied for redatuming and imaging purposes. Claerbout (1968) and Schuster (2009) show how the Green's function on the earth's surface could be obtained by autocorrelating traces generated by buried sources. Wapenaar (2002) proves Claerbout's conjecture by applying Green's theorem and provides a solid mathematical foundation for the further development in interferometry.

In the efforts of applying refraction data for imaging near surface structures, Mallinson (2011) proposes a super-virtual interferometric approach to enhance the SNR for far offset refractions. Zhang and Toksöz (1997) develop a refraction traveltime migration approach that images a refractor. Wang and Zhang (2017) extend the traveltime method to multiple refractors. Hill (1987) applies a wide-angle extrapolator to image two opposite refraction wavefields. Zhang (2006) proposes a method to convert refraction wavefields to virtual reflections by interferometry and then migrate virtual reflections in depth. In this study, we apply the refraction migration method by Zhang (2006) to image a deep refraction interface with long-offset data acquired in Xinjiang, China, for which the deep reflections are entirely missing in the data due to near surface scattering effects.

Method

First, we shall briefly introduce the algorithm of refraction migration method. Following figure shows the schematic raypath of two reciprocal refractions.

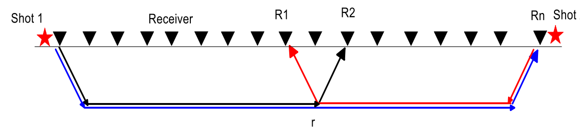

Figure 1: The schematic raypath of two reciprocal refractions. After applying the interferometry, we virtually transform refractions to a series of virtual reflections between R1 and R2.

According to Zhang (2006), the interferometry processing includes two steps. As Figure 1 shows, we want to derive a reflection with a raypath from receiver R1 to R2, the traveltime of this raypath can be formulated as

$$\begin{aligned} T_{refl} &= T_{R1} + T_{R2} - T_{12}, \\ &= T_{R1} - (T_{12} - T_{R2}), \end{aligned} \tag{1}$$

where T_{refl} is the reflection traveltime from receiver R1 to R2 via r, T_{R2} and T_{R1} are the refraction traveltimes from Shot 1 to receiver R2 and from Shot 2 to receiver R1, respectively. T_{12} is the total refraction traveltime from Shot 1 to Shot 2. Then the virtual reflection wavefield can be generated as

$$G(T_{12} - T_{R2}) = G(T_{R2}) \otimes G(T_{12}), \tag{2}$$

$$G(T_{refl}) = G(T_{12} - T_{R2}) \otimes G(T_{R1}), \tag{3}$$

where G is the wavefield for each traveltime. Therefore, the virtual reflection gathers can be created by two steps. First, the last trace of Shot 1 is correlated with every trace in Shot 1, which should create the temporary record as $G(T_{12} - T_{R2})$. Then, each trace in the reversed Shot 2 is correlated with the temporary records on the right side of the trace. Then there should be one trace in the results representing R1 to R2 reflection from the refractor interface.

After the above procedure, we create the interferometric gathers that include both true and false reflection events. According to the stationarity condition, applying PSDM with these gathers should eliminate the false events, since only the true reflection events are coherent.

Reflections from the deep subsurface are often too weak, refraction migration by way of interferometry may offer an alternative solution. Before applying refraction migration, we can apply the super-virtual interferometry approach proposed by Bharadwaj (2011) to enhance the far offset refractions. The enhanced procedure is formulated as

$$G(B|A)^{super} \approx 2ik \int G(B|x')^{vir} \cdot G(A|x')d^2x', \quad (4)$$

where $G(B|A)^{super}$ is the super-virtual trace obtained by convolving the record data $G(A|x')$ with the virtual data $G(B|x')^{vir}$.

Synthetic tests

(1) The window selection for correlation

In the interferometry calculation, the refraction migration method requires more calculation time when processing data with longer offset.

As Figure 1 shows, after the interferometry processing, we virtually move the shot to the position of each receiver. Therefore, when we apply the refraction migration method to long-offset data, each virtual gather shall contain a large number of traces, which lead to a large computation of the prestack depth migration. However, the valid reflection is only received within a limited offset. Therefore, we need to select a proper size of window for correlation to reduce the calculation time and improve the feasibility of the refraction migration method.

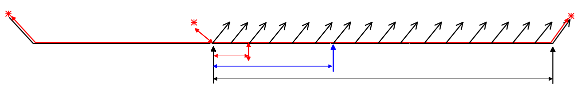

Figure 2: Schematic of the correlation windows. The red, blue, and black lines show three different sizes of windows for correlation.

Figure 2 shows three different sizes of windows. Once the correlation window is determined, we only need to perform interferometry with the traces within the window. We apply a one-layer horizontal model to demonstrate the reliability of this idea. We first design a refractor at the depth of 500 m. The velocities of the first and second layers are 1000 m/s and 2000 m/s, respectively.

Then we determine the critical offset of the true reflection (461.9 m from Snell's law), which is between the 11th and 12th receivers. The sizes of the three correlation windows are 15, 12, and 9 traces, respectively. Figures 3, 4, and 5 show the imaging results and the computation time.

As is shown in Figure 4, when the size of the correlation window is 12 traces, we find that the image is consistent with the true position of the refractor, and the computation time is less than that with 15 traces. Figure 5 shows that the artifacts shall appear when the window is 9 traces.

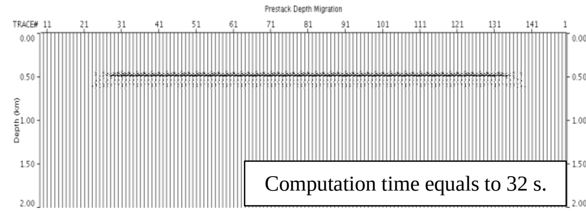

Figure 3: The imaging result of the correlation window with 15 traces.

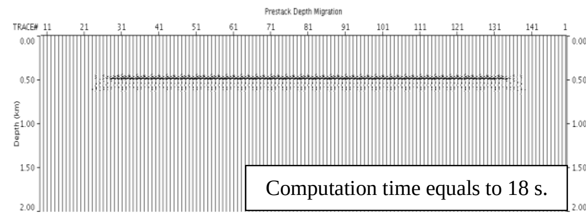

Figure 4: The imaging result of the correlation window with 12 traces.

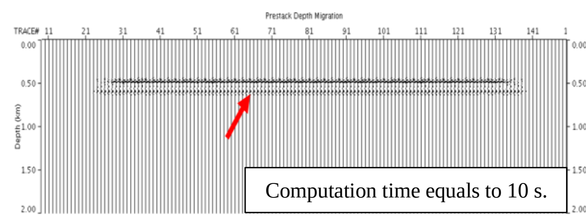

Figure 5: The imaging result of the correlation window with 9 traces. The red arrow indicates the artificial noise.

Therefore, we should select a proper size of correlation window, which is larger than the critical offset of the reflection, to avoid the artifacts and reduce the computation time simultaneously. In this study, we apply the ray tracing theory to obtain the proper window size before applying the interferometry.

(2) Data quality versus imaging results

In the refraction migration method, we obtain the virtual reflections by interferometry. However, the interferometry is sensitive to the correlated signals. Therefore, we design a synthetic test to show how the raw refraction signals affect the final image quality. We first design a horizontal refractor model and apply the refraction migration to obtain the original imaging result. When the random noises are added to the raw refraction signals, the unfocused energy shall appear around the refractor. The final results are shown in Figure 7 and Figure 8. We find that the imaging quality is sensitive to the raw refraction data and the refraction migration method may be failed when the refraction signal is too weak or missing. Therefore, signal enhancement processing of the refraction is necessary before applying the refraction migration method. In this study, we apply super-virtual interferometry to enhance far offset refractions.

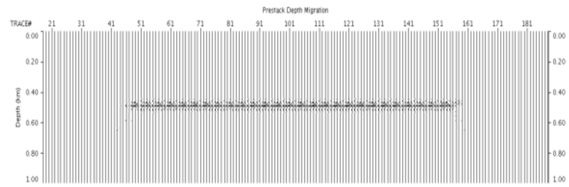

Figure 6: The original imaging result of the refraction migration.

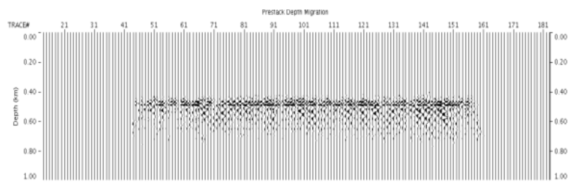

Figure 7: The imaging result when the SNR of refraction equals to 2.

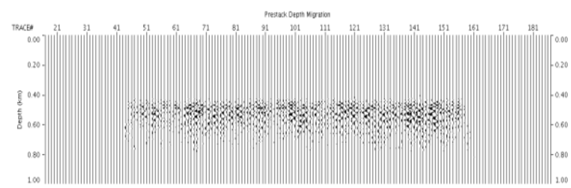

Figure 8: The imaging result when the SNR of refraction equals to 1.

Real data application

We apply the refraction migration method to process a real dataset, for which the deep reflections are entirely missing in the data. The real dataset is acquired with a long-offset geometry in Xinjiang, China. The maximum offset of this dataset is about 50 kilometers and the survey geometry map is shown in Figure 9.

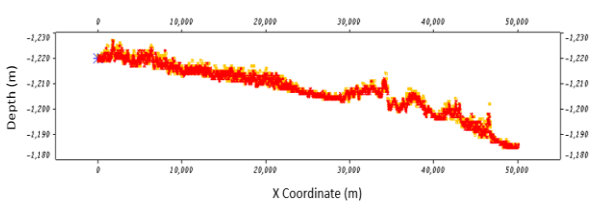

Figure 9: The survey geometry map of the real dataset. The red and yellow points denote the positions of the shots and receivers, respectively.

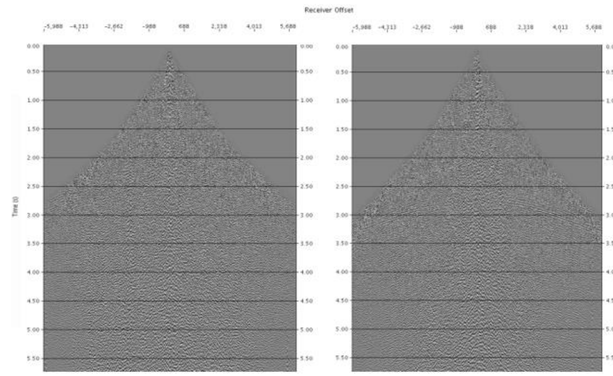

Figure 10: Two processed CMP gathers from the real data.

Figure 10 shows two processed CMP gathers from the real data, for which the deep reflections are entirely missing. Therefore, we utilize the refraction migration to image the deep interface in this area. Before applying the refraction migration, we first perform the super-virtual interferometry to enhance the far offset refractions. Figure 11 shows the partial record of one shot in the real data. The far offset refraction indicates a low SNR. Figure 12 shows that after the super-virtual interferometry is applied, the far offset refraction is enhanced.

We pick the first-arrival traveltime and perform the tomography to obtain the depth-velocity model for prestack depth migration. Then we apply the refraction migration method to image the refraction interface.

In this case, we select 26 couples of the reciprocal shots to perform the refraction migration. The correlated window is 400 traces. The final image result is generated by stacking the images from each couple. Figure 13 shows the refractor image of the real data. We find the depth of the refractor is about 5 km below the surface. Then we overlay the image with the depth-velocity model. Figure 14 demonstrates that the model is consistent with the migration image.

Therefore, we can utilize the refraction migration method to process long-offset data, especially when reflections of the data are too weak or missing, since refractions are almost always available.

Real data application with refraction migration

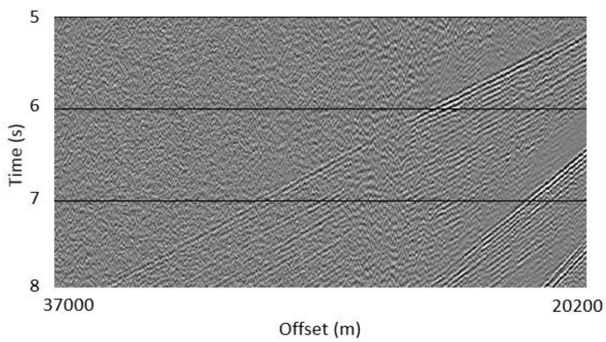

Figure 11: Partial record of one shot in the raw data.

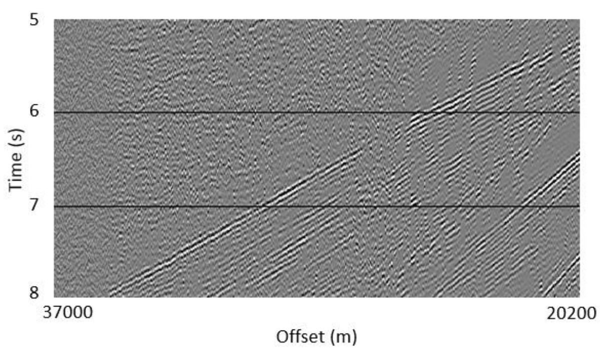

Figure 12: The enhanced refraction after applying the super-virtual interferometry.

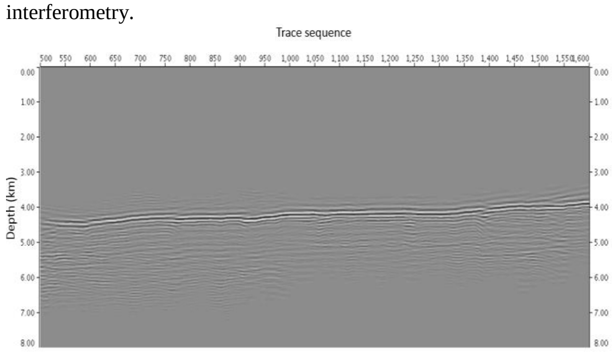

Figure 13: The prestack depth migration result of the real dataset.

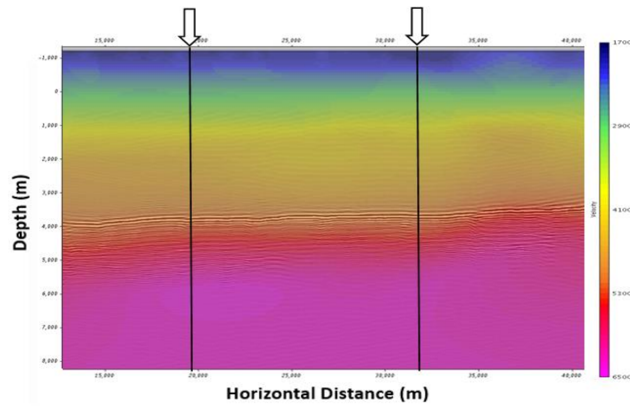

Figure 14: The overlaid model and migration image. The black lines indicate the CMP locations of Figure 11.

Conclusions

In this study, we apply the refraction migration method to image the deep interface in Xinjiang, China. Although the deep reflections of the data are missing, the refraction migration helps to produce a major interface. If data quality is too poor, the imaging results are not going to be reliable. The super-virtual interferometry is applied to enhance the far offset refractions before creating the virtual reflections. Both synthetic and real data tests demonstrate that this method is useful.

Acknowledgments

We thank the financial support from Major State Research Development Program of China under grant No. 2016YFC0601100. We also express our sincere gratitude and thanks to GeoTomo for guidance.